Presynaptic D2 Dopamine Receptors Control LTD Expression and Memory Processes in the Temporal Hippocampus

Jill Rocchetti, Elsa Isingrini, Gregory Dal Bo, Sara Sagheby, Aurore Menegaux, François Tronche, Daniel Levesque, Luc Moquin, Alain Gratton, Tak Pan Wong, et al.

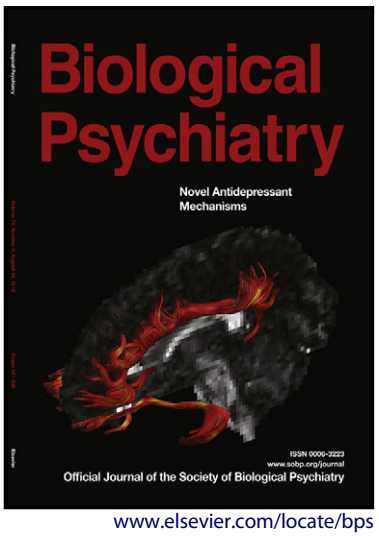

www.elsevier.com/locate/bps

Presynaptic D2 Dopamine Receptors Control LTD Expression and Memory Processes in the Temporal Hippocampus

Jill Rocchetti, Elsa Isingrini, Gregory Dal Bo, Sara Sagheby, Aurore Menegaux, François Tronche, Daniel Levesque, Luc Moquin, Alain Gratton, Tak Pan Wong, Marcelo Rubinstein, Bruno Giros

PII: S0006-3223(14)00166-8
DOI: http://dx.doi.org/10.1016/j.biopsych.2014.03.013
Reference: BPS12167

To appear in: *Biological Psychiatry*

Received date: 22 January 2014
Revised date: 4 March 2014
Accepted date: 13 March 2014

Cite this article as: Jill Rocchetti, Elsa Isingrini, Gregory Dal Bo, Sara Sagheby, Aurore Menegaux, François Tronche, Daniel Levesque, Luc Moquin, Alain Gratton, Tak Pan Wong, Marcelo Rubinstein, Bruno Giros, Presynaptic D2 Dopamine Receptors Control LTD Expression and Memory Processes in the Temporal Hippocampus, *Biological Psychiatry*, http://dx.doi.org/10.1016/j.biopsych.2014.03.013

Presynaptic D2 Dopamine Receptors Control LTD Expression and Memory Processes in the Temporal Hippocampus

Jill Rocchetti*[1], Elsa Isingrini*[1], Gregory Dal Bo*[1], Sara Sagheby[1], Aurore Menegaux[1], François Tronche[2], Daniel Levesque[3], Luc Moquin[1], Alain Gratton[1], Tak Pan Wong[1], Marcelo Rubinstein[4] and Bruno Giros°[1,2]

[1] Department of Psychiatry, Douglas Mental Health University Institute, McGill University, Montreal, Quebec, H4H 1R3, Canada
[2] INSERM, UMRS 1130; CNRS, UMR 8246; Sorbonne University UPMC, Neuroscience Paris-Seine, F-75005, Paris, France
[3] Département de Pharmacie, Université de Montréal, Montréal, Québec, Canada
[4] Instituto de Investigaciones en Ingeniería Genética y Biología Molecular, CONICET and Dept. Fisiología, Biología Molecular y Celular, FCEyN, Universidad de Buenos Aires, Argentina

* Equal contribution
° Corresponding author: bruno.giros@mcgill.ca

Keywords: D2 dopamine receptors | Antipsychotics | LTD | Neuronal plasticity | Temporal hippocampus | Memory

Words in the abstract:	250
Words in the text:	4000
Tables:	0
Figures:	6
Supplemental information:	1 (5 Figures, 3 Tables)

Abstract:

BACKGROUND: Dysfunctional mesocorticolimbic dopamine (DA) signaling has been linked to alterations in motor and reward-based functions associated with psychiatric disorders. Converging evidence from psychiatric patients and use of antipsychotics suggest that misbalance of DA signaling deeply alters hippocampal functions. However, given the lack of full characterization of a functional mesohippocampal pathway, the precise role of DA transmission in memory deficits associated with these disorders and their dedicated therapies is unknown. In particular, the positive outcome of antipsychotic treatments, commonly antagonizing D2 dopamine receptors (D2R), on cognitive deficits and memory impairments remains questionable.

METHODS: Following pharmacological and genetic manipulation of dopamine transmission, we combined anatomical, neurochemical, electrophysiological and behavioral investigations to uncover the role of dopamine D2-like receptors in hippocampal-dependent plasticity and learning. Naïve mice (n=4-21) were used in the different procedures.

RESULTS: We report that DA modulated the both long-term potentiation (LTP) and depression (LTD) in the temporal hippocampus as well as spatial and recognition learning and memory in mice through D_2 dopamine receptors (D2R). Whereas genetic deletion or pharmacological blockade of D2R led to the loss of LTP expression, the specific genetic removal of presynaptic D2R specifically impairs LTD as well as the performances on spatial memory tasks.

CONCLUSION: The pre-synaptic D2Rs in DA fibers of the temporal hippocampus tightly modulate LTD expression and plays a major role in the regulation of hippocampal learning and memory. This direct role of mesohippocampal DA input uncovered here adds a new dimension to DA involvement in the physiology underlying neuropsychiatric disorders deficits.

Introduction

In addition to its roles in motor and reward systems (1, 2), DA has also been acknowledged to be essential in adaptive behaviors, such as attention, learning and memory (3-5). The development of powerful genetic tools has enabled a better understanding of DA's function in the basal ganglia and the cortical structures (6) involved in these motor and reward functions. However, the limited innervation by DA terminals and the low levels of DA receptor (DAR) expression in the hippocampus (7-9) have slowed our understanding of DA's potential role in the mesohippocampal pathway (10). Considering the pathological imbalance in hippocampal DA transmission observed in schizophrenic patients (11-14) and the lack of perspective on the impact of antipsychotic treatments in memory processes, there is an urgent need to better understand the DA contribution in hippocampal-related processes.

Long-term synaptic plasticity, with its two counterparts, LTP and LTD, is underlying neuronal circuit tuning. It was shown 40 years ago that microelectrophoretical application of DA in the hippocampal CA3 region of cats depressed glutamate-induced cell firing (15). However, how DA modulates glutamatergic transmission in the hippocampus is still poorly understood.

Five DARs have been identified in mammals (16) and classified into the D1/D5 - "D1-like" - and D2/D3/D4 - "D2-like" families. Both D1-like and D2-like receptor agonists and antagonists regulate synaptic plasticity (17), but if the role of D1-like receptors in hippocampal synaptic plasticity is quite well understood, little is known about the precise role of the D2R. D1-like receptor blockade inhibits the expression and maintenance of late LTP (18-20), whereas the D1-like agonist SKF-38393 favored the early and late phases of LTP (21, 22). Accordingly, D1KO mice showed an absence of late LTP *in vitro* (23) and exhibited impaired spatial memory (24). Conversely, the role of D2-like receptors in hippocampus remains controversial. Activation of D2R would exert a suppressive effect on CA1 LTD in the rat hippocampus (25) with no effect on LTP (21), but D2 agonists directly administered in the hippocampus improved memory performances in radial maze tasks (26, 27). Rats treated with the D2R antagonist haloperidol displayed spatial learning deficits (28, 29) and impaired recognition memory (30, 31). Systemic injection of the D2/D3 antagonist sulpiride affected learning in the

spatial version of the Morris water maze (MWM) (32), but whether it is a specific effect on the hippocampus remains unclear (33).

Whereas D1-like receptors are only present on dopaminoceptive neurons, D2R are localized both post-synaptically where they activate multiple signalization pathways (34) and pre-synaptically where they exert an inhibitory control over DA synthesis and release (35, 36). This dual localization of D2R potentially results in multi-modal processes with complex effects.

Here, we showed that D2R post-synaptic expression was restricted to neurons of the dentate gyrus (DG), whereas DA fibers expressing the dopamine transporter (DAT) originating from the VTA and carrying pre-synaptic D2R innervated the temporal CA1 areas. The genetic deletion of D2R severely impairs both NMDAR-dependent LTP and LTD in CA1, matching with remodeling of mesohippocampal DA fibers and decrease in performance on learning and memory tasks. The pharmacological blockade of D2R in naïve mice reproduced these impairments. Finally, the specific genetic deletion of pre-synaptic D2R resulted in deficits of both LTD expression and spatial memory without impairing LTP levels.

Material and Methods

Detailed procedures are listed in the supplemental information section.

Animals: Mice with a constitutive deletion of the D2R were from the Jackson Laboratories (B6.129S2-*Drd2*^{tm1Low}/J), D2cre mice were from Gensat (MMRC; B6.FVB(Cg)-Tg(Drd2-cre)$^{ER44Gsat/Mmucd}$) and crossed with mice carrying ROSA-tomato reporter from Jackson Laboratories (Gt(ROSA)26Sor$^{tm9(CAG-tdTomato)Hze}$), mice with floxed D2R gene (36) and DATcre mice (37) were directly obtained.

Anatomical procedures: DAR mRNAs were detected by radioactive and fluorescent *in situ* hybridization. Immunolabeling was adapted from previous protocol to detect DAT, CaMK2α, TH and GABA on coronal slices from D2KO, D2^{DATcre} and sulpiride-treated mice. All experiments were performed on naïve mice (n=4-10; Sup Table 1).

Electrophysiological recordings: Field excitatory postsynaptic potentials (fEPSP) and whole-cell patch-clamp recordings were performed on coronal slices prepared from D2KO, D2^{DATcre} and C57Bl/6 WT mice in presence of sulpiride or SCH23390. All experiments were done in the presence of 5 µM bicuculline. All experiments were performed on naïve mice (n=6-11; Sup Table 2).

Behavioral tests: Males D2KO, D2^{DATcre}, sulpiride treated (i.p.: 50mg/kg; intra-HP: 2.5µg) and their respective controls, were exposed to spatial and cued versions of the MWM, Barnes maze, two objects recognition, contextual and cued fear conditioning. Only naive mice were tested. All experiments were performed on naïve mice (n=9-21; Sup Table 3).

Statistical comparisons: Results are reported as mean ± SEM. Statistical analysis were made with Student's t test and ANOVA, unless otherwise specified (see Statistical tables Sup 1, 2 and 3).

Results

Mapping of DA receptors and fibers in the hippocampal formation

The distribution of the five DAR was evaluated by *in situ* hybridization in C57BL/6 mouse brains **(Figure 1A-C, Figure sup 1).** D3R and D4R mRNA expression in the hippocampus **(Figure sup 1B-C)** fell below our detection limit **(Figure sup 1B)**. D1R mRNA expression was restricted to the granular cell layer of the DG **(Figure sup 1A)**, and D2R mRNA expression was observed only in the polymorphic layer (hilus) of the DG **(Figure 1A-B).** D5R mRNA was expressed in granular and pyramidal cell layers **(Figure sup 1D).** Radiolabeling with [I^{125}]-iodosulspride the presence of D2R in the granular cell layer, in addition to the polymorphic layer of the DG **(Figure 1D-E).** The specificity of D2R expression was shown using D2KO mice **(Figure 1C-1F)**. Combined fluorescent D2R *in situ* hybridization and immunolabeling against CaMKIIα showed the D2R-expressing neurons in the hilus to be glutamatergic **(Figure 1G-I, Figure sup 1E-H)**. Using reporter tdTomato^{D2cre} mice, we identify these neurons as mossy neurons, given their morphology and their projection patterns **(Figure 1J)**.

As most of the tyrosine hydroxylase (TH) labeling found in hippocampus originates from noradrenergic neurons (38), we visualized DAT^+ fibers to characterize the DA projections. DAT^+ fibers were restricted to the temporal area of CA1 **(Figure 1K-L)** and totally absent in the septal part of the hippocampus **(Figure sup 2A-B)**. The strongest labeling was observed in the dorsal part of the *stratum radiatum* and the ventral part of the *lacunosum moleculare* (LMol) of CA1 **(Figure sup 2C-D)**. The specificity of DAT labeling was confirmed using DATKO mice (38) **(Figure sup 2E)**.

Constitutive deletion of D2Rs led to a profound remodeling of the VTA-hippocampus dopaminergic pathway

D2KO mice had three- to seven-fold more DAT^+ fibers in the hippocampus than WT animals **(Figure 2A-C)**. In the LMol layer of CA1, D2KO mice showed three-fold increase in DAT^+ fibers (n=4; 337±52) compared to WT (n=4; 111±30). The *radiatum* layer showed a similar increase (308±50 in D2KO ; 85±12 in D2WT), and a major sprouting was observed in the *oriens* and pyramidal cell layers, with seven-fold more

DAT^+ fibers (257±42) in D2KO than in D2WT mice (38±9). Interestingly, whereas DAT^+ fibers were absent in the hilus of the DG in D2WT animals, they were visible in D2KO mice (32.3±12.2). No DAT^+ fibers were observable in any other subdivisions of the temporal hippocampus or in septal areas.

To determine the origin of DAT^+ fibers increase, we injected fluorescent retrobeads into the CA1 of D2KO and D2WT mice **(Figure 2C-D and Figure sup 2E-E'')**. The majority of retrogradely labeled neurons were localized in the VTA (87-89%), only a fraction of them were DAergic (16-21%), whereas the majority was GABAergic (79-84%). The number (n=27) and the proportion (21%) of TH^+ neurons in D2KO mice were slightly increased, compared to WT (n=22; 16%). Thus, this increase did not account for the massive sprouting observed in D2KO hippocampus. Furthermore, DA levels in the temporal hippocampus were significantly higher in D2KO mice (293.9±30.9 ng/g) compared to D2WT mice (169.9±21.4 ng/g) **(Figure 2E; Figure sup 2G)**. Finally, we assessed by microdialysis whether this increased sprouting of DA terminals in temporal hippocampus would translate into an increase in KCl-induced DA release **(Figure 2F; Figure sup 2F)**. Basal levels of extracellular DA were similar in D2WT and D2KO mice. However, KCl-induced paired depolarization led to 2.4 times greater DA release in the D2KO mice (K1=23.0±6.3 ng/ml; K2=31.5±10.4 ng/ml) compared to WT littermates (K1=11.2±2.2; K2=13.05±2.6). The second KCl-induced stimulation (K2) in D2KO mice resulted in a 1.4-fold increase in DA release, compared to the first depolarization (K1), which was significantly higher than that observed in D2WT mice (1.16), implying the absence of inhibitory control from the presynaptic D2Rs upon DA release **(Figure 2F)**.

Constitutive deletion of the D2 receptor impaired synaptic plasticity in the temporal CA1

We examined whether remodeling of the VTA-hippocampus dopaminergic pathway in D2KO mice would impair N-methyl-D-aspartate receptor (NMDAR)-dependent synaptic plasticity in CA1. In the dorsal area of temporal CA1, where DAT^+ fibers were detected, high-frequency stimulation induced a significant LTP in D2WT animals (n=6; 1.44±0.06) but not in D2KO mice (n=8; 1.15±0.07) **(Figure 3A)**. For LTD expression, paired-pulse low-frequency stimulation induced stable depression in the D2WT (n=9;

0.83±0.04), but not in D2KO slices (n=7; 1.08±0.04) **(Figure 3B)**. This reduction in long-term synaptic plasticity could be due to a change in glutamatergic transmission; in voltage clamp configuration, we recorded miniature excitatory post-synaptic currents (mEPSC) in glutamatergic pyramidal neurons of temporal CA1 in D2KO (n=11) and D2WT (n=11) mice at -80 mV, in the presence of tetrodotoxin (TTX) **(Figure 3C)**. Neither the frequency (D2WT: 0.25±0.02 Hz; D2KO: 0.28±0.04 Hz) nor the amplitude (D2WT: 7.44±0.42 pA; D2KO: 6.92±0.49 pA) of the mEPSCs were modified, suggesting that neither the glutamate spontaneous release nor post-synaptic glutamate sensitivity was altered in CA3-CA1 synapses **(Figure 3D)**. Paired-pulse facilitation of fEPSPs at CA3-CA1 glutamatergic synapses at increasing inter-pulse intervals was also conserved in D2KO brain slices **(Figure 3E).** However, fEPSPs recorded in the D2KO mice (n=10) were significantly larger in the medium range than in D2WT (n=8), revealing an increased excitability of CA3-CA1 synapses **(Figure 3F)**. We wondered whether the increased DA released in D2KO mice would overactivate postsynaptic D5Rs expressed at CA1 glutamatergic cells and produce deficits in synaptic plasticity. The D1/D5 antagonist SCH23390 (1 µM, 30 min) reinstated HFS-induced LTP on D2KO slices to a level comparable to D2WT slices (n=9; 1.37±0.06) **(Figure 3G),** whereas it had no effect on the LTP induced in D2WT slices (n=6; 1.40±0.09) **(Figure sup 3A**). Nonetheless, SCH23390 application (1 µM, 40 min) did not affect the level of LTD in D2KO slices (n=6; 1.04±0.05) **(Figure 3H)**.

Constitutive deletion of the D2 receptor caused spatial and recognition-memory deficits

In the spatial version of the MWM, D2KO mice were unable to learn the platform location. The mean latency during the last training session was significantly longer in D2KO mice (72.4±7.4 s) compared to D2WT (38.5±8.9 s). During the challenge session performed 90 min after the final training, D2KO mice (23±4.7%) spent significantly less time in the active quadrant than WT (43.8±2.2%), suggesting impairments in short-term spatial memory **(Figure 4A)**. This deficit contrasted with the normal performance of D2KO mice in the cued version of the MWM **(Figure 4B)**, where no differences in escape latencies were observed between the D2KO (day 5: 25.4±5.4) and D2WT (day

5: 22.5±5.4). In the spatial Barnes maze, D2KO acquired properly the escape hole location during training but did not significantly visit the active quadrant during the challenge session performed 24 hrs after the last training (D2WT: 35.5±4; D2KOs: 21.6±4.5), suggesting long-term spatial memory impairments **(Figure 4C)**. Recognition memory was also impaired in the two-object recognition task, D2KO mice exhibited significantly decreased percentages of time spent exploring the new object compared to WT (D2KOs: 53.1±4%; D2WT: 65.2±3.8%) **(Figure 4D)**. Finally, D2KO mice exhibited no impairment in the fear-conditioning paradigm **(Figure sup 4)**.

Pharmacological blockade of the D2Rs produced a loss of spatial memory and of synaptic plasticity in the hippocampus

Given the possible compensatory mechanisms that could occurred during D2KO mouse development, we tested pharmacological blockade of D2Rs in naïve C57BL/6J animals.

Daily systemic administration of the D2/D3R antagonist sulpiride (50 mg/kg) 30 minutes before the first of two training sessions in the spatial version of the MWM revealed a slow-onset effect. During the first 4 training days, the escape latency in the sulpiride group (58.3±11 s) and the NaCl group (50.3±5.4 s) were identical. However, within subsequent trainings, sulpiride-treated mice became slower to find the platform location (sulpiride: 70.2±10.6 s; control: 39.6±7.3 s), and spent less time in the active quadrant (sulpiride: 21.1±10.4%; control: 42.6±4.1%) during the challenge **(Figure 5A)**. When the sulpiride treatment started 1 week before the MWM training and was maintained during the procedure, the mice were unable to learn the platform location (sulpiride: 71.1±9.5 s; control: 44.1±10.1 s) and spent significantly less time in the active quadrant during the challenge (sulpiride: 17.5±3.7%; control: 42.6±4.1%) **(Figure 5B)**. Interestingly, if the sulpiride pre-treatment was stopped prior to the MWM training, the deficit during the first 3 days of training (sulpiride: 80.4±5.9 s; control: 60±4.6 s) disappeared during the last days (sulpiride: 44.1±10.1 s; control: 39.6±7.3 s) and the challenge (sulpiride: 36±4.9%; control: 42.6±4.1%) **(Figure 5C)**.

To assess the acute effects of D2R blockade on synaptic plasticity, we applied sulpiride (10 µM) to C57BL/6J slices during LTP and LTD induction. Sulpiride application produced the same impairment pattern observed in D2KO slices. Both LTP (n=7; 1.55±0.1) and LTD (n=7; 0.78±0.08) were observed in the untreated slices, whereas sulpiride produced a significant decrease in LTP (n=8; 1.30±0.06) **(Figure 5D)** and abolition of LTD expression (n=6; 1.03±0.05) **(Figure 5E)**.

As in D2KO mice, C57Bl/6J mice treated for 15 days with sulpiride showed a highly significant sprouting (1.3-1.7 fold more) of DAT^+ fibers in LMol (Sulpiride: 132.3±22.5 ; control: 99.1±10.6), *Radiatum* (Sulpiride: 126.7±5.9; control: 76.2±5.9) and Pyramidal/*oriens* (Sulpiride: 51.1±6.4; control: 32.7±2.2) layers **(Figure 5F and sup 2H-H')**. Dopamine levels were also increased in treated mice (Sulpiride: 204.4±20.1 ng/g; vs control:169.8±12.4 ng/g), attesting the fast remodelling of DA system in hippocampus **(Figure 5G and sup 2I)**.

To undoubtedly associate the effects of D2R blockade with hippocampal-dependent processes, we implanted bilateral cannulas into the temporal part of the hippocampi of C57BL/6J mice **(Figure sup 2J)**. Direct sulpiride infusion (5 µg/µl, 0.1 µl/side), initiated 1 week before the MWM procedure and maintained during training, reproduced the learning deficit observed in D2KO mice **(Figure 5H)**. The final escape latency was significantly increased in sulpiride-treated mice (77.3±6.6 s) compared to control mice (29±7.5 s), and the time spent in the active quadrant was significantly decreased (19.6±3.9%) compared to controls (33.2±4.1%).

D2R deletion in DAT^+ neurons was sufficient to impair LTD expression and spatial memory formation in the hippocampus

To specifically assess the contribution of pre-synaptic D2Rs we crossed *Drd2*$^{loxP/loxP}$ mice (36) with BAC-DATicre mice (37) to remove D2 autoreceptors in DAT^+ neurons **(Figure sup 5A-C**). Pre-synaptic knockout of the D2R gene ($D2^{DATcre}$ mice) had no effect on the expression of LTP in CA1 (n=8; 1.40±0.05) in comparison with WT^{DATcre} animals (n=6; 1.44±0.06) **(Figure 6A)**. Conversely, $D2^{DATcre}$ mice totally loss their LTD expression (n=6; 1.06±0.05) compared to WT^{DATcre} mice (n=9; 0.83±0.04), **(Figure 6B)**. Remarkably, the input-output relationship in evoked glutamatergic fEPSPs was not

different between the $D2^{DATcre}$ mice and their WT^{DATcre} littermates **(Figure 6C)**. To assess whether this LTD deficit could be a consequence of pre-synaptic D2R absence on DA release and synthesis, we analyzed DAT^+ fibers density and DA tissue levels in the temporal hippocampus of $D2^{DATcre}$ mice. We found that $D2^{DATcre}$ mice exhibited 3.3 and 7.5 fold more DAT^+ fibers in the *radiatum* ($D2^{DATcre}$: 228.3±55.6; WT^{DATcre}: 68.4±12.5) and in the *oriens*/pyramidal cell layers ($D2^{DATcre}$: 221.8±64.9; WT^{DATcre}: 29.4±15.3), respectively, compared to WT^{DATcre} littermates, with no changes in the LMol layer ($D2^{DATcre}$: 81.5±17.3; WT^{DATcre}: 89.2±33.9) **(Figure 6E)**. Finally, we observed a significant 1.3-fold increase in tissue DA levels in the $D2^{DATcre}$ mice's temporal hippocampus compared to WT^{DATcre} mice **(Figure 6F, Figure sup 5E)**.

The $D2^{DATcre}$ mice exhibited dramatic memory impairments in the spatial version of the MWM. The final mean escape latency was significantly increased in the $D2^{DATcre}$ (50.9±11.2s) compared to WT^{DATcre} (21.8±8.8s) and the percentage of time spent in the active quadrant was significantly decreased in $D2^{DATcre}$ (22.4±6.7%) compared to WT^{DATcre} mice (44.2±3.9%) **(Figure 6G)**. Further linking the LTD role in these memory deficits, while blockade of D1-like receptors with SCH23390 rescued HFS induced LTP expression in D2KO slices, it had no effect neither on LTD deficits nor on memory deficits (**Figure 3H and sup 3B**).

Discussion

The organization of the dopamine circuitry in the hippocampus suggests a tonic functional mode of transmission

We localized DAR expressing cells using sensitive *in situ* hybridization techniques; D5R mRNA expression in the entire granular cell layer of the DG and the pyramidal cell layer of CA1 and CA3, and D1R expression restricted to the granular cells of the DG confirm previous reports in rats and primates (39-43). We could not detect D3R or D4R transcript expression in the hippocampus: D3 mRNA was observed only in the amygdalohippocampal area (44), but the absence of D4 mRNA detection contrasts with its previously described participation in CA1 synapses depotentiation through CA3 GABAergic interneurons (45, 46). mRNA localization and binding experiments showed

the restricted expression of D2R in the hilus, as well as in the DG, flanking the granular cell layer. Furthermore, as D2Rs binding was detectable in the hippocampus of $D2^{DATcre}$ mice (**Figure sup 5D**), it clearly indicated that the labeling in the DG mostly originated from the hilar D2-positive cells. The demonstration that D2mRNA co-localized with CaMKIIα in the hilus confirmed the recent report of putative D2R expression in mossy cells using Drd2-EGFP transgenic mice (47). Morphological characteristics of these cells confirmed that these were glutamate mossy interneurons (48-50).

Dopaminergic innervation, assessed by DAT expression, was restricted to the temporal area of CA1. The organization of the DA system, with an absence of DAT^+ fibers in the polymorphic layers of the DG, is typical of a volume transmission *modus operandi* (51-53). Retrograde labeling with fluorobeads injected into the temporal hippocampus confirmed results obtained in rats (54), we showed about 20% of the efferent VTA neurons are TH^+ neurons and identified all other projecting neurons as GABAergic. Using *in vivo* microdialysis, we showed that the functionally releasable pool of DA is under the control of pre-synaptic D2 activation, as described in the striatum (35, 36). The presynaptic D2Rs conferred to DA neurons a high structural plasticity, as shown by the massive sprouting of these DAT-positive fibers in the D2KO, $D2^{DATcre}$ mice and following a chronic treatment with sulpiride. This observation is in accordance with previous studies reporting that D2R activation exerted an inhibitory effect on DA sprouting in the striatum (55, 56). Therefore, the upregulation of DAT fibers, DA tissue and DA release levels suggest that chronic use of antipsychotics could produce drastic anatomical changes in the hippocampus.

Dopamine D2 receptors control the plasticity of the temporal hippocampus

The potential role played by D2Rs in the modulation of long-term hippocampal synaptic plasticity was poorly documented (21, 25). Our anatomical description emphasized a critical role for pre-synaptic D2R in DAT fiber architecture in the temporal region. Therefore, we focused on this region to investigate the role of D2R activation in synaptic plasticity.

In D2KO mice, we observed a suppression of both LTP and LTD after HFS or paired-pulse LFS of the Schaffer collaterals in temporal CA1. As it was previously

reported regarding cortico-striatal plasticity (57), no critical changes in basal glutamatergic transmission were detected. Because we could not detect post-synaptic D2R expression in CA1, we assumed that D5R overactivation at glutamatergic cells was potentially involved. Interestingly, blocking D1-like receptors with SCH23390 in D2KO slices reestablished LTP levels but did not restore LTD. Functional response of D1Rs activation has been shown to follow an “inverted U-shape” curve in the prefrontal cortex (58). Our results suggested that this model is relevant regarding LTP expression at glutamatergic synapses of CA1 but that LTD expression responds to different mechanisms.

The impairments in LTP and LTD were almost entirely replicated by application in C57BL/6J mice slices of sulpiride that has high specificity for D2/D3 receptors (59). In particular, LTD was fully blocked as reported in D2KO mice. These results showed that D2Rs played a pivotal role in the expression of CA3-CA1 plasticity.

Dopamine D2 receptors control spatial learning in the temporal hippocampus

Given the drastic changes in synaptic plasticity and the dopaminergic circuit remodeling observed in D2KO and sulpiride-treated mice, we anticipated downstream functional impairments in hippocampus-dependent learning and memory processes. Systemic administration of D2-like antagonists in rats had been shown to trigger learning and memory deficits (28, 30, 32, 60-62). Accordingly, the profound deficits in both LTP and LTD observed in D2KO mice were associated with dramatic impairments in three hippocampus-dependent learning and memory paradigms: the spatial MWM, the Barnes maze and the NORT. The absence of deficits in the cued version of the MWM, known to involve mainly striatal DA regulation (63, 64) implied an absence of sensorimotor deficits in the D2KO strain.

The experiments using various treatment times with Sulpiride provided greater insight into the rapid dynamics of changes that occur after D2R blockade and revealed a reversible adaptive response controlled by D2R activity. This observation is consistent with the rapid onset of the beneficial effects of antipsychotics on positive symptoms of schizophrenia in human patients (65).

Finally, stereotaxic administration of sulpiride into the temporal hippocampi of C57BL/6J animals fully replicated the learning deficit observed in D2KO mice. This unambiguously demonstrated the specific participation of D2Rs localized in the temporal hippocampus in the MWM performance.

Specific deletion of pre-synaptic D2Rs is correlated with LTD absence in the temporal hippocampus and learning deficits

In $D2^{DATcre}$ mice, with pre-synaptic D2R deletion, a dichotomy between LTP and LTD expression was observed, LTP expression remaining intact whereas LTD was abolished. Strikingly, performance in the spatial MWM was equally impaired in $D2^{DATcre}$ and in D2KO mice. LTP and LTD operate by different molecular mechanisms, with potentially distinct roles (66, 67). In particular, LTD has been shown to be essential for spatial memory consolidation (68), novel spatial learning (69) and behavioral flexibility (70). NMDAR-LTD in the hippocampus relies on phosphatase activity (71), whereas the expression of NMDAR-LTP is dependent upon the postsynaptic activation of calcium/calmodulin-dependent kinase II (CaMKII) and trafficking of GluA1 containing AMPARs (72). Notably, the activity of the G protein-independent glycogen synthase kinase-3beta (GSK3β)/Akt pathway might be required in NMDAR-dependent LTD expression in the hippocampus (73, 74). In the mouse striatum, D2R activation is essential for Akt inhibition and GSK3β activation (7, 75), therefore the recruitment of these pathways in D2-dependent plasticity in the hippocampus remains to be investigated.

Another interesting question is the function of D2Rs expressed in the mossy cells of the DG. Whereas it is unlikely that these postsynaptic D2Rs would be implicated in LTD and spatial memory deficits, because they are intact in $D2^{DATcre}$ mice, they might participate in the deficit of LTP expression of D2KO mice through a modulation of CA3 to CA1 excitability.

Overall, our data uncover that LTD expression in the temporal hippocampus plays a determinant role in the regulation of learning and memory and that pre-synaptically expressed D2Rs in DA fibers tightly modulate this aspect of hippocampus function. On

the one hand, D2Rs control synaptic and extrasynaptic DA levels, DA innervation, LTD expression thresholds and learning and memory performance through their presynaptic location in temporal CA1. On the other hand, they seem to be implicated in LTP modulation through postsynaptic D1R overactivation. Even if a clarification of the mechanisms involved in these processes is still necessary, these contributions were largely underestimated until now. The functional role of VTA dopaminergic input in the hippocampus potentially shapes a complex circuitry when added to the loop from the hippocampus to the nucleus accumbens and then to the VTA, which has been shown to control the firing of DA neurons (10, 76). The existence of a direct mesohippocampal functional DA pathway and the role of pre-synaptic D2R are therefore key elements to consider in the etiology of psychotic symptoms and the long-term effects of antipsychotic treatments, including their potential impact on hippocampal volume in schizophrenic patients (77) and the role of DA in aberrant salience and the etiology of delusions (78).

Acknowledgements: BG is a Canadian Research Chair in the Neurobiology of Mental Disorders. GDB and EI are supported by a postdoc grant from the FRQS. This work was supported by the Canada Research Chairs program (BG), the Canadian Foundation for Innovation and the Graham Boeckh Foundation for Schizophrenia Research (BG). We thank Ms Erika Vigneault and Marie-Eve Desaulnier for excellent care and maintenance of all mice colonies.

Financial disclosure: All authors report no biomedical financial interests or potential conflicts of interest.

Bibliography

1. Beninger RJ (1983): The role of dopamine in locomotor activity and learning. *Brain Res*. 287:173-196.
2. Wise RA, Rompre PP (1989): Brain dopamine and reward. *Annual review of psychology*. 40:191-225.
3. Cools R (2006): Dopaminergic modulation of cognitive function-implications for L-DOPA treatment in Parkinson's disease. *Neurosci Biobehav Rev*. 30:1-23.
4. Nieoullon A (2002): Dopamine and the regulation of cognition and attention. *Prog Neurobiol*. 67:53-83.
5. Weinberger DR, Berman KF, Chase TN (1988): Mesocortical dopaminergic function and human cognition. *Annals of the New York Academy of Sciences*. 537:330-338.
6. Tritsch NX, Sabatini BL (2012): Dopaminergic modulation of synaptic transmission in cortex and striatum. *Neuron*. 76:33-50.
7. Beaulieu JM, Del'guidice T, Sotnikova TD, Lemasson M, Gainetdinov RR (2011): Beyond cAMP: The Regulation of Akt and GSK3 by Dopamine Receptors. *Front Mol Neurosci*. 4:38.
8. Gasbarri A, Sulli A, Packard MG (1997): The dopaminergic mesencephalic projections to the hippocampal formation in the rat. *Progress in neuro-psychopharmacology & biological psychiatry*. 21:1-22.
9. Swanson LW (1982): The projections of the ventral tegmental area and adjacent regions: a combined fluorescent retrograde tracer and immunofluorescence study in the rat. *Brain Res Bull*. 9:321-353.
10. Lisman JE, Pi HJ, Zhang Y, Otmakhova NA (2010): A thalamo-hippocampal-ventral tegmental area loop may produce the positive feedback that underlies the psychotic break in schizophrenia. *Biol Psychiatry*. 68:17-24.
11. Boyer P, Phillips JL, Rousseau FL, Ilivitsky S (2007): Hippocampal abnormalities and memory deficits: new evidence of a strong pathophysiological link in schizophrenia. *Brain Res Rev*. 54:92-112.
12. Folley BS, Astur R, Jagannathan K, Calhoun VD, Pearlson GD (2010): Anomalous neural circuit function in schizophrenia during a virtual Morris water task. *Neuroimage*. 49:3373-3384.
13. Hanlon FM, Weisend MP, Hamilton DA, Jones AP, Thoma RJ, Huang M, et al. (2006): Impairment on the hippocampal-dependent virtual Morris water task in schizophrenia. *Schizophr Res*. 87:67-80.
14. Ledoux A-A, Phillips JL, Labelle A, Smith A, Bohbot VD, Boyer P (2013): Decreased fMRI activity in the hippocampus of patients with schizophrenia compared to healthy control participants, tested on a wayfinding task in a virtual town. *Psy Res Neuroimaging*. 211:47-56.
15. Biscoe TJ, Straughan DW (1966): Micro-electrophoretic studies of neurones in the cat hippocampus. *J Physiol*. 183:341-359.
16. Beaulieu JM, Gainetdinov RR (2011): The physiology, signaling, and pharmacology of dopamine receptors. *Pharmacol Rev*. 63:182-217.
17. Jay TM (2003): Dopamine: a potential substrate for synaptic plasticity and memory mechanisms. *Prog Neurobiol*. 69:375-390.
18. Frey U, Matthies H, Reymann KG, Matthies H (1991): The effect of dopaminergic D1 receptor blockade during tetanization on the expression of long-term potentiation in the rat CA1 region in vitro. *Neurosci Lett*. 129:111-114.
19. Lemon N, Manahan-Vaughan D (2006): Dopamine D1/D5 receptors gate the acquisition of novel information through hippocampal long-term potentiation and long-term depression. *J Neurosci*. 26:7723-7729.
20. Lisman J, Grace AA, Duzel E (2011): A neoHebbian framework for episodic memory; role of dopamine-dependent late LTP. *Trends in neurosciences*. 34:536-547.

21. Huang YY, Kandel ER (1995): D1/D5 receptor agonists induce a protein synthesis-dependent late potentiation in the CA1 region of the hippocampus. *Proc Natl Acad Sci U S A*. 92:2446-2450.
22. Otmakhova NA, Lisman JE (1996): D1/D5 dopamine receptor activation increases the magnitude of early long-term potentiation at CA1 hippocampal synapses. *J Neurosci*. 16:7478-7486.
23. Matthies H, Becker A, Schroeder H, Kraus J, Hollt V, Krug M (1997): Dopamine D1-deficient mutant mice do not express the late phase of hippocampal long-term potentiation. *Neuroreport*. 8:3533-3535.
24. El-Ghundi M, Fletcher PJ, Drago J, Sibley DR, O'Dowd BF, George SR (1999): Spatial learning deficit in dopamine D(1) receptor knockout mice. *Eur J Pharmacol*. 383:95-106.
25. Chen Z, Ito K, Fujii S, Miura M, Furuse H, Sasaki H, et al. (1996): Roles of dopamine receptors in long-term depression: enhancement via D1 receptors and inhibition via D2 receptors. *Receptors Channels*. 4:1-8.
26. Packard MG, White NM (1991): Dissociation of hippocampus and caudate nucleus memory systems by posttraining intracerebral injection of dopamine agonists. *Behav Neurosci*. 105:295-306.
27. Wilkerson A, Levin ED (1999): Ventral hippocampal dopamine D1 and D2 systems and spatial working memory in rats. *Neuroscience*. 89:743-749.
28. Terry AV, Jr., Hill WD, Parikh V, Evans DR, Waller JL, Mahadik SP (2002): Differential effects of chronic haloperidol and olanzapine exposure on brain cholinergic markers and spatial learning in rats. *Psychopharmacology (Berl)*. 164:360-368.
29. Terry AV, Jr., Parikh V, Gearhart DA, Pillai A, Hohnadel E, Warner S, et al. (2006): Time-dependent effects of haloperidol and ziprasidone on nerve growth factor, cholinergic neurons, and spatial learning in rats. *J Pharmacol Exp Ther*. 318:709-724.
30. Schroder N, de Lima MN, Quevedo J, Dal Pizzol F, Roesler R (2005): Impairing effects of chronic haloperidol and clozapine treatment on recognition memory: possible relation to oxidative stress. *Schizophr Res*. 73:377-378.
31. Ozdemir H, Ertugrul A, Basar K, Saka E (2012): Differential effects of antipsychotics on hippocampal presynaptic protein expressions and recognition memory in a schizophrenia model in mice. *Progress in neuro-psychopharmacology & biological psychiatry*. 39:62-68.
32. Stuchlik A, Rehakova L, Telensky P, Vales K (2007): Morris water maze learning in Long-Evans rats is differentially affected by blockade of D1-like and D2-like dopamine receptors. *Neurosci Lett*. 422:169-174.
33. Setlow B, McGaugh JL (1998): Sulpiride infused into the nucleus accumbens posttraining impairs memory of spatial water maze training. *Behav Neurosci*. 112:603-610.
34. Bonci A, Hopf FW (2005): The dopamine D2 receptor: new surprises from an old friend. *Neuron*. 47:335-338.
35. Anzalone A, Lizardi-Ortiz JE, Ramos M, De Mei C, Hopf FW, Iaccarino C, et al. (2012): Dual control of dopamine synthesis and release by presynaptic and postsynaptic dopamine D2 receptors. *J Neurosci*. 32:9023-9034.
36. Bello EP, Mateo Y, Gelman DM, Noain D, Shin JH, Low MJ, et al. (2011): Cocaine supersensitivity and enhanced motivation for reward in mice lacking dopamine D2 autoreceptors. *Nat Neurosci*. 14:1033-1038.
37. Turiault M, Parnaudeau S, Milet A, Parlato R, Rouzeau JD, Lazar M, et al. (2007): Analysis of dopamine transporter gene expression pattern -- generation of DAT-iCre transgenic mice. *Febs J*. 274:3568-3577.
38. Giros B, Jaber M, Jones SR, Wightman RM, Caron MG (1996): Hyperlocomotion and indifference to cocaine and amphetamine in mice lacking the dopamine transporter. *Nature*. 379:606-612.

39. Bergson C, Mrzljak L, Smiley JF, Pappy M, Levenson R, Goldman-Rakic PS (1995): Regional, cellular, and subcellular variations in the distribution of D1 and D5 dopamine receptors in primate brain. *J Neurosci*. 15:7821-7836.
40. Ciliax BJ, Nash N, Heilman C, Sunahara R, Hartney A, Tiberi M, et al. (2000): Dopamine D(5) receptor immunolocalization in rat and monkey brain. *Synapse*. 37:125-145.
41. Fremeau RT, Jr., Duncan GE, Fornaretto MG, Dearry A, Gingrich JA, Breese GR, et al. (1991): Localization of D1 dopamine receptor mRNA in brain supports a role in cognitive, affective, and neuroendocrine aspects of dopaminergic neurotransmission. *Proc Natl Acad Sci U S A*. 88:3772-3776.
42. Levey AI, Hersch SM, Rye DB, Sunahara RK, Niznik HB, Kitt CA, et al. (1993): Localization of D1 and D2 dopamine receptors in brain with subtype-specific antibodies. *Proc Natl Acad Sci U S A*. 90:8861-8865.
43. Tiberi M, Jarvie KR, Silvia C, Falardeau P, Gingrich JA, Godinot N, et al. (1991): Cloning, molecular characterization, and chromosomal assignment of a gene encoding a second D1 dopamine receptor subtype: differential expression pattern in rat brain compared with the D1A receptor. *Proc Natl Acad Sci U S A*. 88:7491-7495.
44. Kato K, Masa T, Tawara Y, Kobayashi K, Oka T, Okabe A, et al. (2001): Dendritic aberrations in the hippocampal granular layer and the amygdalohippocampal area following kindled-seizures. *Brain Res*. 901:281-295.
45. Andersson RH, Johnston A, Herman PA, Winzer-Serhan UH, Karavanova I, Vullhorst D, et al. (2012): Neuregulin and dopamine modulation of hippocampal gamma oscillations is dependent on dopamine D4 receptors. *Proc Natl Acad Sci U S A*. 109:13118-13123.
46. Kwon OB, Paredes D, Gonzalez CM, Neddens J, Hernandez L, Vullhorst D, et al. (2008): Neuregulin-1 regulates LTP at CA1 hippocampal synapses through activation of dopamine D4 receptors. *Proc Natl Acad Sci U S A*. 105:15587-15592.
47. Gangarossa G, Longueville S, De Bundel D, Perroy J, Herve D, Girault JA, et al. (2012): Characterization of dopamine D1 and D2 receptor-expressing neurons in the mouse hippocampus. *Hippocampus*. 22:2199-2207.
48. Amaral DG, Scharfman HE, Lavenex P (2007): The dentate gyrus: fundamental neuroanatomical organization (dentate gyrus for dummies). *Progress in brain research*. 163:3-22.
49. Jinde S, Zsiros V, Jiang Z, Nakao K, Pickel J, Kohno K, et al. (2012): Hilar mossy cell degeneration causes transient dentate granule cell hyperexcitability and impaired pattern separation. *Neuron*. 76:1189-1200.
50. Scharfman HE, Myers CE (2012): Hilar mossy cells of the dentate gyrus: a historical perspective. *Frontiers in neural circuits*. 6:106.
51. Descarries L, Watkins KC, Garcia S, Bosler O, Doucet G (1996): Dual character, asynaptic and synaptic, of the dopamine innervation in adult rat neostriatum: a quantitative autoradiographic and immunocytochemical analysis. *J Comp Neurol*. 375:167-186.
52. Rice ME, Cragg SJ (2008): Dopamine spillover after quantal release: rethinking dopamine transmission in the nigrostriatal pathway. *Brain Res Rev*. 58:303-313.
53. Zoli M, Jansson A, Sykova E, Agnati LF, Fuxe K (1999): Volume transmission in the CNS and its relevance for neuropsychopharmacology. *Trends Pharmacol Sci*. 20:142-150.
54. Gasbarri A, Verney C, Innocenzi R, Campana E, Pacitti C (1994): Mesolimbic dopaminergic neurons innervating the hippocampal formation in the rat: a combined retrograde tracing and immunohistochemical study. *Brain Res*. 668:71-79.
55. Parish CL, Stanic D, Drago J, Borrelli E, Finkelstein DI, Horne MK (2002): Effects of long-term treatment with dopamine receptor agonists and antagonists on terminal arbor size. *Eur J Neurosci*. 16:787-794.

56. Tripanichkul W, Stanic D, Drago J, Finkelstein DI, Horne MK (2003): D2 Dopamine receptor blockade results in sprouting of DA axons in the intact animal but prevents sprouting following nigral lesions. *Eur J Neurosci*. 17:1033-1045.
57. Calabresi P, Saiardi A, Pisani A, Baik JH, Centonze D, Mercuri NB, et al. (1997): Abnormal synaptic plasticity in the striatum of mice lacking dopamine D2 receptors. *J Neurosci*. 17:4536-4544.
58. Vijayraghavan S, Wang M, Birnbaum SG, Williams GV, Arnsten AF (2007): Inverted-U dopamine D1 receptor actions on prefrontal neurons engaged in working memory. *Nat Neurosci*. 10:376-384.
59. Caley CF, Weber SS (1995): Sulpiride: an antipsychotic with selective dopaminergic antagonist properties. *The Annals of pharmacotherapy*. 29:152-160.
60. Ertugrul A, Ozdemir H, Vural A, Dalkara T, Meltzer HY, Saka E (2011): The influence of N-desmethylclozapine and clozapine on recognition memory and BDNF expression in hippocampus. *Brain Res Bull*. 84:144-150.
61. Ploeger GE, Spruijt BM, Cools AR (1992): Effects of haloperidol on the acquisition of a spatial learning task. *Physiol Behav*. 52:979-983.
62. Prokopova I, Bahnik S, Doulames V, Vales K, Petrasek T, Svoboda J, et al. (2012): Synergistic effects of dopamine D2-like receptor antagonist sulpiride and beta-blocker propranolol on learning in the carousel maze, a dry-land spatial navigation task. *Pharmacology, biochemistry, and behavior*. 102:151-156.
63. Morris RG, Anderson E, Lynch GS, Baudry M (1986): Selective impairment of learning and blockade of long-term potentiation by an N-methyl-D-aspartate receptor antagonist, AP5. *Nature*. 319:774-776.
64. Teather LA, Packard MG, Smith DE, Ellis-Behnke RG, Bazan NG (2005): Differential induction of c-Jun and Fos-like proteins in rat hippocampus and dorsal striatum after training in two water maze tasks. *Neurobiol Learn Mem*. 84:75-84.
65. Agid O, Kapur S, Arenovich T, Zipursky RB (2003): Delayed-onset hypothesis of antipsychotic action: a hypothesis tested and rejected. *Arch Gen Psychiatry*. 60:1228-1235.
66. Holscher C (1999): Synaptic plasticity and learning and memory: LTP and beyond. *Journal of neuroscience research*. 58:62-75.
67. Kemp A, Manahan-Vaughan D (2004): Hippocampal long-term depression and long-term potentiation encode different aspects of novelty acquisition. *Proc Natl Acad Sci U S A*. 101:8192-8197.
68. Ge Y, Dong Z, Bagot RC, Howland JG, Phillips AG, Wong TP, et al. (2010): Hippocampal long-term depression is required for the consolidation of spatial memory. *Proc Natl Acad Sci U S A*. 107:16697-16702.
69. Goh JJ, Manahan-Vaughan D (2012): Spatial Object Recognition Enables Endogenous LTD that Curtails LTP in the Mouse Hippocampus. *Cereb Cortex*.
70. Nicholls RE, Alarcon JM, Malleret G, Carroll RC, Grody M, Vronskaya S, et al. (2008): Transgenic mice lacking NMDAR-dependent LTD exhibit deficits in behavioral flexibility. *Neuron*. 58:104-117.
71. Luscher C, Malenka RC (2012): NMDA receptor-dependent long-term potentiation and long-term depression (LTP/LTD). *Cold Spring Harb Perspect Biol*. 4.
72. Selcher JC, Xu W, Hanson JE, Malenka RC, Madison DV (2012): Glutamate receptor subunit GluA1 is necessary for long-term potentiation and synapse unsilencing, but not long-term depression in mouse hippocampus. *Brain Res*. 1435:8-14.
73. Peineau S, Nicolas CS, Bortolotto ZA, Bhat RV, Ryves WJ, Harwood AJ, et al. (2009): A systematic investigation of the protein kinases involved in NMDA receptor-dependent LTD: evidence for a role of GSK-3 but not other serine/threonine kinases. *Mol Brain*. 2:22.
74. Peineau S, Taghibiglou C, Bradley C, Wong TP, Liu L, Lu J, et al. (2007): LTP inhibits LTD in the hippocampus via regulation of GSK3beta. *Neuron*. 53:703-717.

75. Beaulieu JM, Tirotta E, Sotnikova TD, Masri B, Salahpour A, Gainetdinov RR, et al. (2007): Regulation of Akt signaling by D2 and D3 dopamine receptors in vivo. *J Neurosci*. 27:881-885.
76. Lisman JE, Grace AA (2005): The hippocampal-VTA loop: controlling the entry of information into long-term memory. *Neuron*. 46:703-713.
77. Ho BC, Andreasen NC, Ziebell S, Pierson R, Magnotta V (2011): Long-term antipsychotic treatment and brain volumes: a longitudinal study of first-episode schizophrenia. *Arch Gen Psychiatry*. 68:128-137.
78. Kapur S (2003): Psychosis as a state of aberrant salience: a framework linking biology, phenomenology, and pharmacology in schizophrenia. *Am J Psychiatry*. 160:13-23.

FIGURE LEGENDS

Figure 1: DA D2 receptors and DA fibers distribution in the hippocampus.
A-C) D2R mRNA expression detected by antisens [^{35}S]-oligonucleotides in hippocampus of WT mice (A,B) was restricted to the polymorphic layer of dentate gyrus along anteroposterior axis. No signal was detected on coronal slices from D2KO mice (C). **D-F)** Autoradiographic detection of D2R using [^{125}I]-iodosulpride labeling in the granular layer of dentate gyrus and in the proximal pyramidal cells of CA3 in WT mice (D,E) with no signal in the D2KO slices (F). **G-I)** Fluorescent *in situ* hybridization for D2R mRNA (G, red) coupled to immunolabeling for CaMK2α (H, green) in mossy cells of dentate gyrus (I) with Hoechst staining (blue).Scale bar=25µm. **J)** Morphological confirmation of mossy cells expressing D2R in D2-tomato reporter mice. Scale bar=25µm. **K)** Schematic 3D representation of mice hippocampus with representation of coronal sections within temporal hippocampus (anterior to bregma, -3.2 mm). **L)** Immunolabeling for DAT (red) positive fibers restricted in CA1 division of mice hippocampus. Slices were counterstained with Hoechst staining (blue). Scale bar=50µm. LMol: *Laconosum Molecular* layer; Rad: *Stratum radiatum*; Pyr: Pyramidal layer.

Figure 2: Anatomical and physiological characterizations of hyperdopaminergia in D2KO mice.
A) Immunolabeling of DAT positive fibers (red) in the *stratum radiatum* layer of the hippocampus of D2WT and D2KO mice. Coronal slices containing the hippocampus were counterstained with Hoescht (blue). Scale bars: 50 µm. **B)** Quantification of DAT+ fibers in CA1 layers (LMol: *Laconosum Molecular* layer; Rad: *Stratum radiatum*; Pyr: Pyramidal layer; Ori: *Oriens*) of the right hippocampus in D2WT and D2KO mice (n=4 for each group; compared to D2WT: **p<0.01). **C)** Schematic representations of retrolabeled neurons distribution in ventral mesencephalon of D2WT (left) and D2KO (right) mice. **D)** Table compiling the numbers and the proportion of DAergic or GABAergic neurons retrogradelly labeled in VTA or SNc in D2WT (n=10) and D2KO (n=10) mice. **E)** HPLC analysis of tissue catecholamine (DA and DOPAC) levels in the hippocampus of D2WT (n=10) and D2KO (n=9) mice (compared to D2WT: **p<0.01). **F) Left,** Microdialysis analysis of extracellular DA in the right temporal hippocampus of D2WT and D2KO mice (n=6 per group) at baseline and during two KCl stimulations (K1, K2). **Center,** Area under the curve during the two KCl-evoked DA release (K1, K2) in D2WT and D2KO mice. **Right,** DA concentration measured by the ratio K2/K1 in D2WT (1.05) and D2KO (1.38) mice (Compared to D2WT: *p<0.05).

Figure 3: Synaptic plasticity of the temporal hippocampus in D2KO mice
A) Left, High frequency induced LTP in D2WT (n=6) and D2KO (n=8) mice hippocampus slices. **Right,** Mean final slope in each genotype (Compared to baseline: ###p<0.001; Compared to D2WT: **p<0.01). **B) Left,** Paired-pulse low frequency induced LTD in D2WT (n=9) and D2KO (n=7) mice hippocampus slices. **Right,** Mean final slope

in each genotype (compared to baseline: $^{\#\#}p<0.01$; compared to D2WT: **p<0.01). **C) Left panel,** Examples of traces of miniature EPSCs recorded in CA1 pyramidal cells of D2WT and D2KO hippocampus at -80mV. **D)** Mean amplitude and frequency of the mEPSCs recorded in D2WT and D2KO slices (n=11 cells in each group). **E)** Paired-pulses facilitation in WT (n=7; 30 ms: 1.58±0.09; 50 ms: 1.50±0.10; 75 ms: 1.44±0.05; 100 ms: 1.37±0.05; 150 ms: 1.32±0.07; 200 ms: 1.27±0.06; 500 ms: 0.97±0.04) and D2KO (n=7; 30 ms: 1.54±0.08; 50 ms: 1.41±0.08; 75 ms: 1.32±0.06; 100 ms: 1.30±0.07; 150 ms: 1.28±0.03; 200 ms: 1.18±0.04; 500 ms: 0.98±0.03) hippocampus slices. **F)** Input-output relationship at CA3-CA1 synapses in WT (n=8) and D2KO (n=10) mice slices (compared to D2WT: ***p<0.001, **p<0.01, *p<0.05). Each recorded fEPSP was normalized by the fEPSP recorded for the maximum intensity of stimulation. **G) Left,** High frequency induced LTP in D2KO mice hippocampus slices after SCH23390 (1 µM, 30 min) application (n=9) compared to untreated D2KO slices (n=8). **Right,** Mean final slope in each condition (compared to baseline: $^{\#\#\#}p<0.001$; compared to untreated slices: *p<0.05). **H) Left,** Paired-pulse low frequency induced LTD in D2KO mice hippocampus slices after SCH23390 (1 µM, 40 min) application (n=6) compared to untreated D2KO slices (n=7). **Right,** Mean final slope in each condition (no significant difference).

Figure 4: Hippocampal-dependent memory performance in the D2KO mice.
A) Left, Mean escape latency in the spatial hidden-platform version of the MWM in D2WT (n=17) and D2KO (n=18) (Compared to D2WT: *p<0.05; ***p<0.001). **Right,** Percentage of time spent in the active quadrant during the probe test of the MWM in each genotype (compared to chance performance of 25%: $^{\#\#}p<0.01$; compared to D2WT: *p<0.05). **B)** Mean escape latency in the Cued version of the MWM for the D2WT (n=16) and the D2KO (n=15) groups. **C) Left,** Escape latency in the spatial Barnes maze in D2WT (n=9) and D2KO (n=10) groups. **Right,** Percentage of time spent in the active quadrant during the probe test of the Barnes maze in each genotype (compared to chance performance of 25%: $^{\#}p<0.05$; compared to D2WT: *p<0.05). **D)** Percentage of time exploring the new object in the novel object recognition task in D2WT (n=9) and D2KO (n=10) (compared to chance performance of 50%: $^{\#\#}p<0.01$; compared to D2WT: *p<0.05).

Figure 5: Spatial memory performance and synaptic plasticity after pharmacological blockage of D2R by sulpiride

A) Left, Mean escape latency in the spatial hidden-platform version of the MWM in Control (NaCl 0.9%, n=21) and Sulpiride (i.p., 50 mg/kg, n=9) treated mice during the 7 days of MWM (compared to Control: *p<0.05; ** p<0.01; ***p<0.001). **Right,** Percentage of time spent in the active quadrant during the probe test of the MWM in each condition (compared to chance performance of 25%: $^{###}$p<0.001; compared to Control: *p<0.05). **B) Left,** Mean escape latency in the spatial hidden-platform version of the MWM in Control (NaCl 0.9%, n=21) and Sulpiride (i.p., 50 mg/kg, n=11) treated mice with treatment started 7 days before the MWM and carried on during the 7 days of experiment (compared to Control: *p<0.05; ** p<0.01; ***p<0.001). **Right,** Percentage of time spent in the active quadrant during the probe test of the MWM in each condition (compared to chance performance of 25%: $^{###}$p<0.001; compared to Control: ***p<0.001). **C) Left,** Mean escape latency in the spatial hidden-platform version of the MWM in Control (NaCl 0.9%, n=21) and Sulpiride (i.p., 50 mg/kg, n=11) treated mice with treatment started 7 days before the MWM but stopped during the 7 days of experiment (compared to day 1: *p<0.05; ***p<0.001). **Right,** Percentage of time spent in the active quadrant during the probe test of the MWM in each condition (compared to chance performance of 25%: $^{#}$p<0.05; $^{###}$p<0.001). **D) Left,** High frequency induced LTP in C57BL/6J mice hippocampus slices after Sulpiride (10 µM, 30 min) application (n=9) compared to untreated slices (n=7). **Right,** Mean of the final slope in each condition (compared to baseline: $^{##}$p<0.01; compared to untreated slices: *p<0.05). **E) Left,** Paired-pulse low frequency induced LTD in C57BL/6J mice hippocampus slices after Sulpiride (10 µM, 40 min) application (n=6) compared to untreated slices (n=8). **Right,** Mean of the final slope in each condition (compared to baseline $^{#}$p<0.05; compared to untreated slices: *p<0.05). **F)** Quantification of DAT+ fibers immunostaining in CA1 layers (LMol: *Laconosum Molecular* layer; Rad: *Stratum radiatum*; Pyr: Pyramidal layer; Ori: *Oriens*) of the right hippocampus in control and Sulpiride-treated mice (n=4 for each group, compared to WT: *p<0.05). **G)** HPLC analysis of tissue catecholamine (DA and DOPAC) levels in the hippocampus of control (n=7) and Sulpiride-treated (n=7) mice (compared to control: *p<0.05). **H) Left,** Mean escape latency in the spatial hidden-platform version of the MWM for Control (NaCl 0.9%; n= 10) and Sulpiride (2.5 µg each side; n=11) injected mice (compared to Control: *p<0.05, ***p<0.005). **Right,** Percentage of time spent in the active quadrant during the probe test of the MWM in each condition (compared to Control: *p<0.05).

Figure 6: Synaptic plasticity, anatomical characterization and spatial memory in presynaptic D2R knock-out mice

A) Left, High frequency induced LTP in WT^{DATCre} (n=6) and $D2^{DATCre}$ (n=9) mice hippocampus slices. **Right,** Mean of the final slope in each genotype (compared to baseline: $^{###}$p<0.001). **B) Left,** Paired-pulse low frequency induced LTD in WT^{DATCre}

(n=7) and $D2^{DATCre}$ (n=6) mice hippocampus slices. **Right,** Mean of the final slope in each genotype (compared to baseline: $^{\#\#}p<0.01$; compared to WT^{DATCre}: $^{**}p<0.01$). **C)** Intensity-amplitude (input-output) relationship at CA3-CA1 synapses in WT^{DATCre} (n=7) and $D2^{DATcre}$ (n=6) mice slices. Each recorded fEPSP was normalized by the fEPSP recorded for the maximum intensity of stimulation. **D)** Image of DAT positive fibers in the *stratum radiatum* layer of the CA1 temporal hippocampus in $D2^{DATcre}$ mice. Scale bar: 50 µm. **E)** Quantification of DAT+ fibers immunostaining in CA1 layers (LMol: *Laconosum Molecular* layer; Rad: *Stratum radiatum*; Pyr: Pyramidal layer; Ori: *Oriens*) of the right hippocampus in WT^{DATCre} and $D2^{DATcre}$ mice (n=4 for each group, compared to WT: $^{*}p<0.05$). **F)** HPLC analysis of tissue catecholamine (DA and DOPAC) levels in the hippocampus of WT^{DATCre} (n=7) and $D2^{DATcre}$ (n=8) mice (compared to WT^{DATCre}: $^{*}p<0.05$). **G) Left,** Mean escape latency in the spatial hidden-platform version of the MWM in WT (n=9) and $D2^{DATcre}$ (n=10) groups (compared to WT^{DATCre}: $^{*}p<0.05$, $^{**}p<0.01$, $^{***}p<0.005$). **Right,** Percentage of time spent in the active quadrant during the probe test of the MWM in each genotype (compared to chance performance of 25%: $^{\#\#\#}p<0.001$; compared to WT^{DATCre}: $^{*}p<0.05$).

Fig. 1

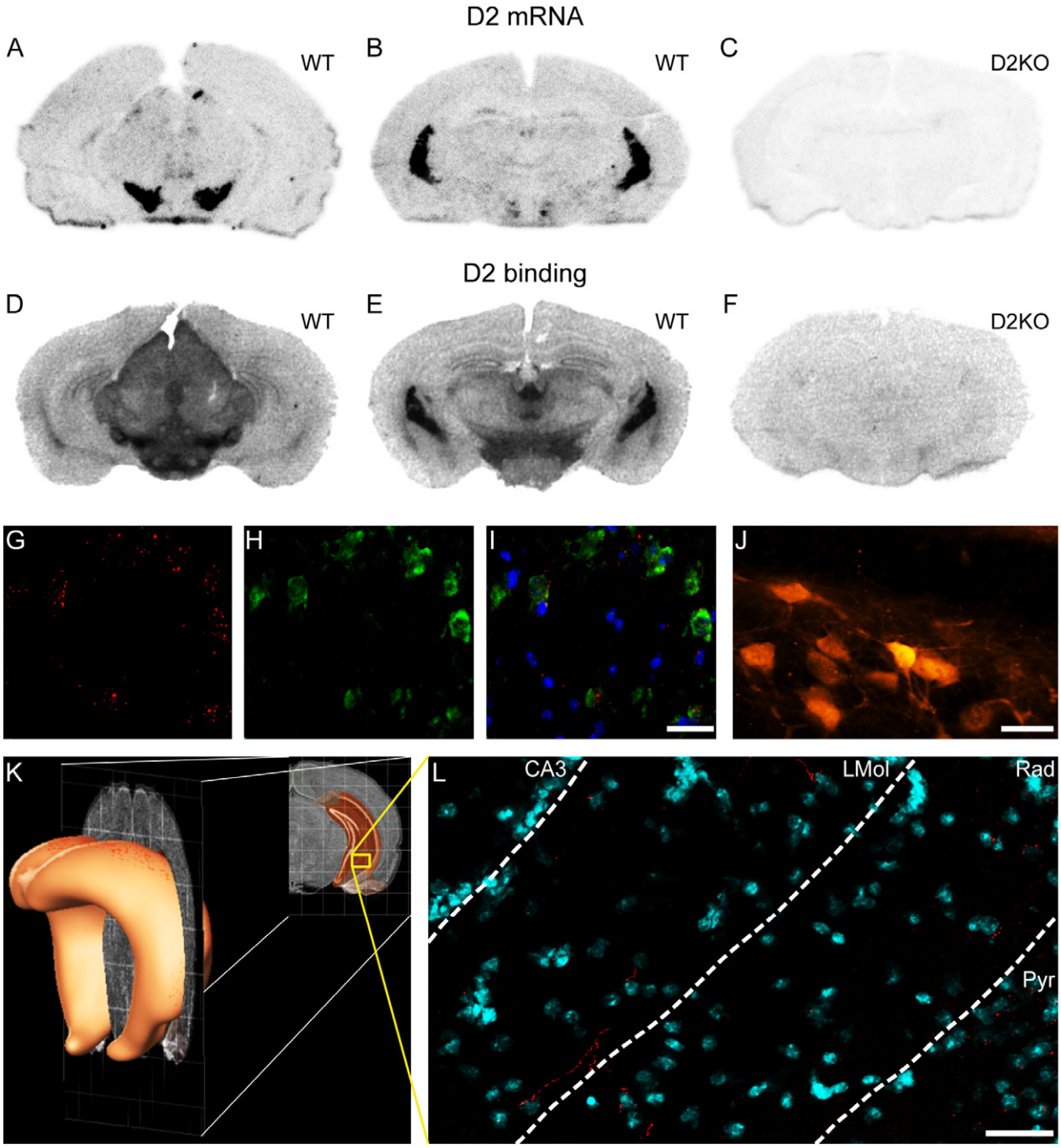
D2 mRNA
A
WT
B
WT
C
D2KO
D2 binding
D
WT
E
WT
F
D2KO
G
H
I
J
K
L
CA3
LMol
Rad
Pyr

Fig. 2

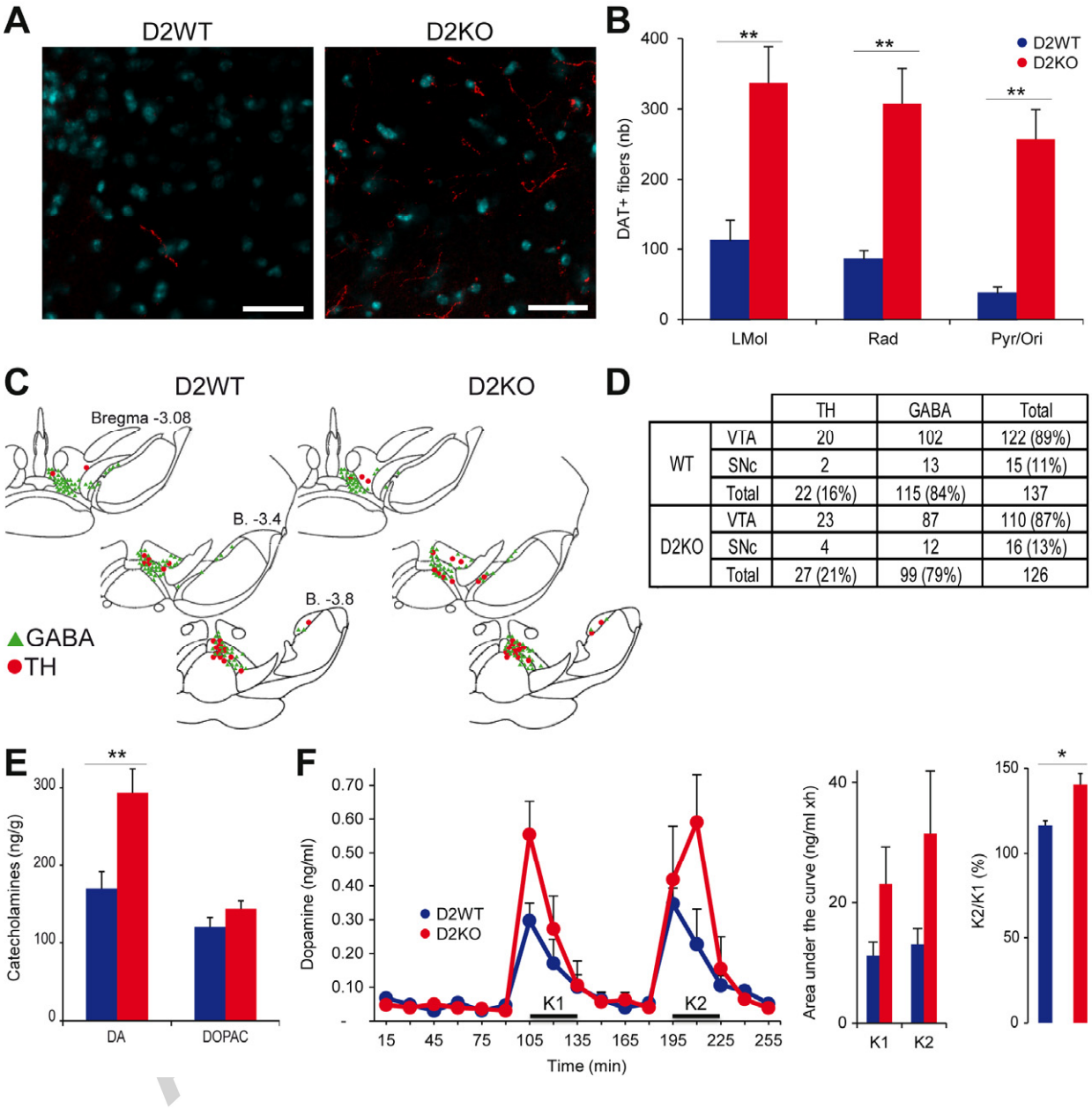

		TH	GABA	Total
WT	VTA	20	102	122 (89%)
	SNc	2	13	15 (11%)
	Total	22 (16%)	115 (84%)	137
D2KO	VTA	23	87	110 (87%)
	SNc	4	12	16 (13%)
	Total	27 (21%)	99 (79%)	126

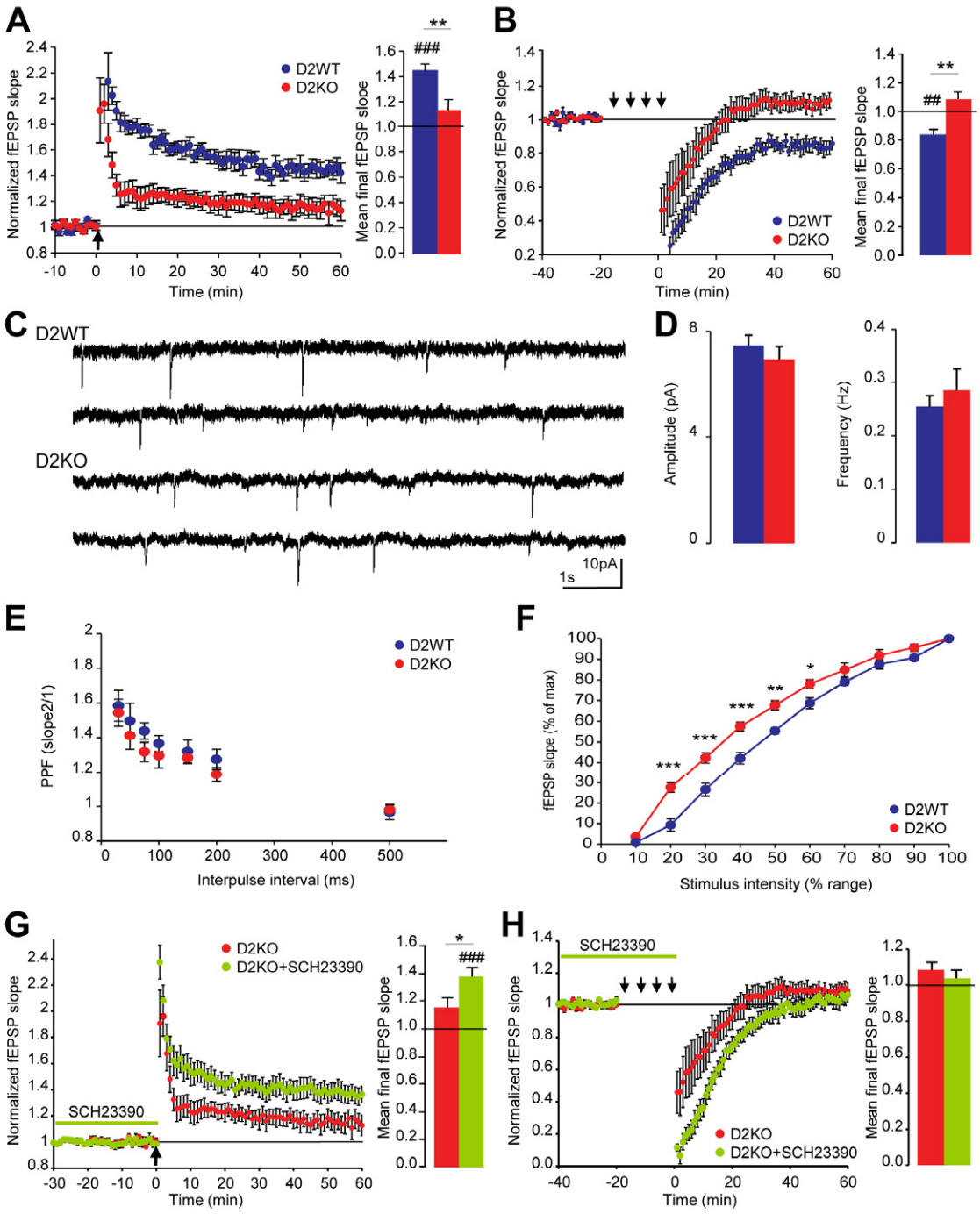
A
Normalized fEPSP slope
Time (min)
D2WT
D2KO
Mean final fEPSP slope
**
###
B
Normalized fEPSP slope
Time (min)
D2WT
D2KO
Mean final fEPSP slope
**
##
C
D2WT
D2KO
10pA
1s
D
Amplitude (pA)
Frequency (Hz)
E
PPF (slope2/1)
Interpulse interval (ms)
D2WT
D2KO
F
fEPSP slope (% of max)
Stimulus intensity (% range)
D2WT
D2KO
*
**
***
***
***
G
Normalized fEPSP slope
Time (min)
SCH23390
D2KO
D2KO+SCH23390
Mean final fEPSP slope
*
###
H
SCH23390
Normalized fEPSP slope
Time (min)
D2KO
D2KO+SCH23390
Mean final fEPSP slope

Fig. 4

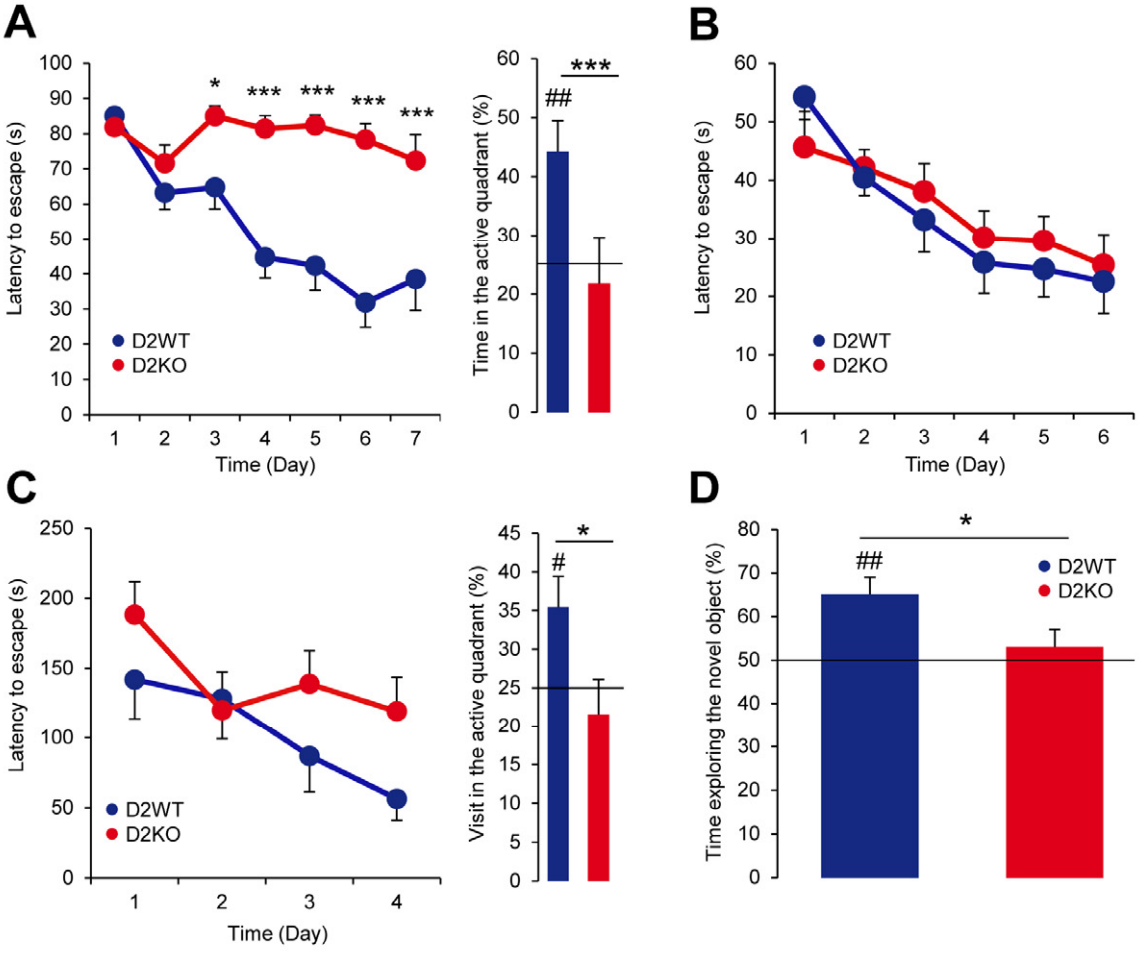

Fig. 5

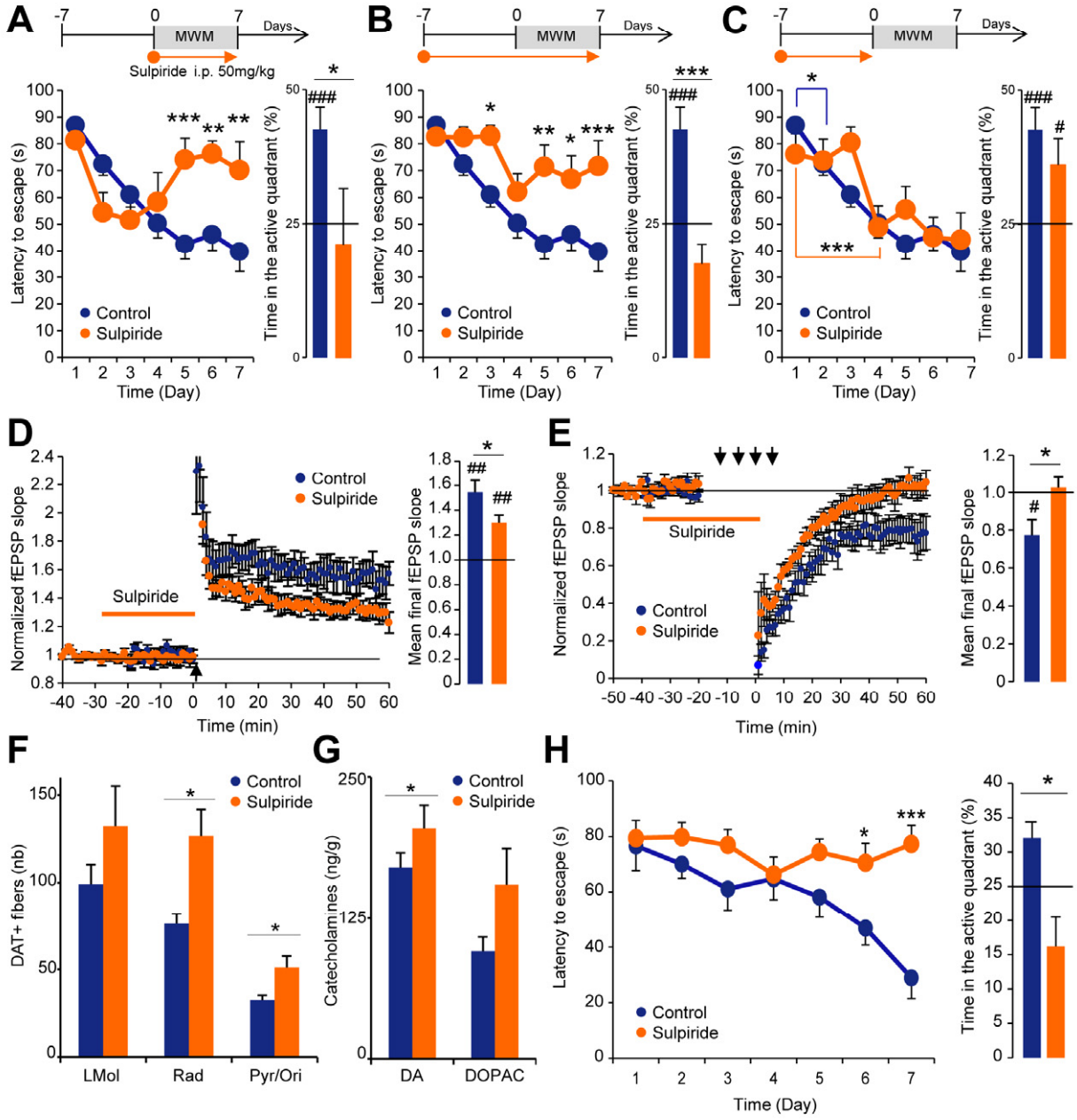
A
B
C
-7
0
7
Days
MWM
Sulpiride i.p. 50mg/kg
Latency to escape (s)
Time (Day)
Control
Sulpiride
Time in the active quadrant (%)
D
Normalized fEPSP slope
Sulpiride
Time (min)
Mean final fEPSP slope
E
F
DAT+ fibers (nb)
LMol
Rad
Pyr/Ori
G
Catecholamines (ng/g)
DA
DOPAC
H

Fig. 6

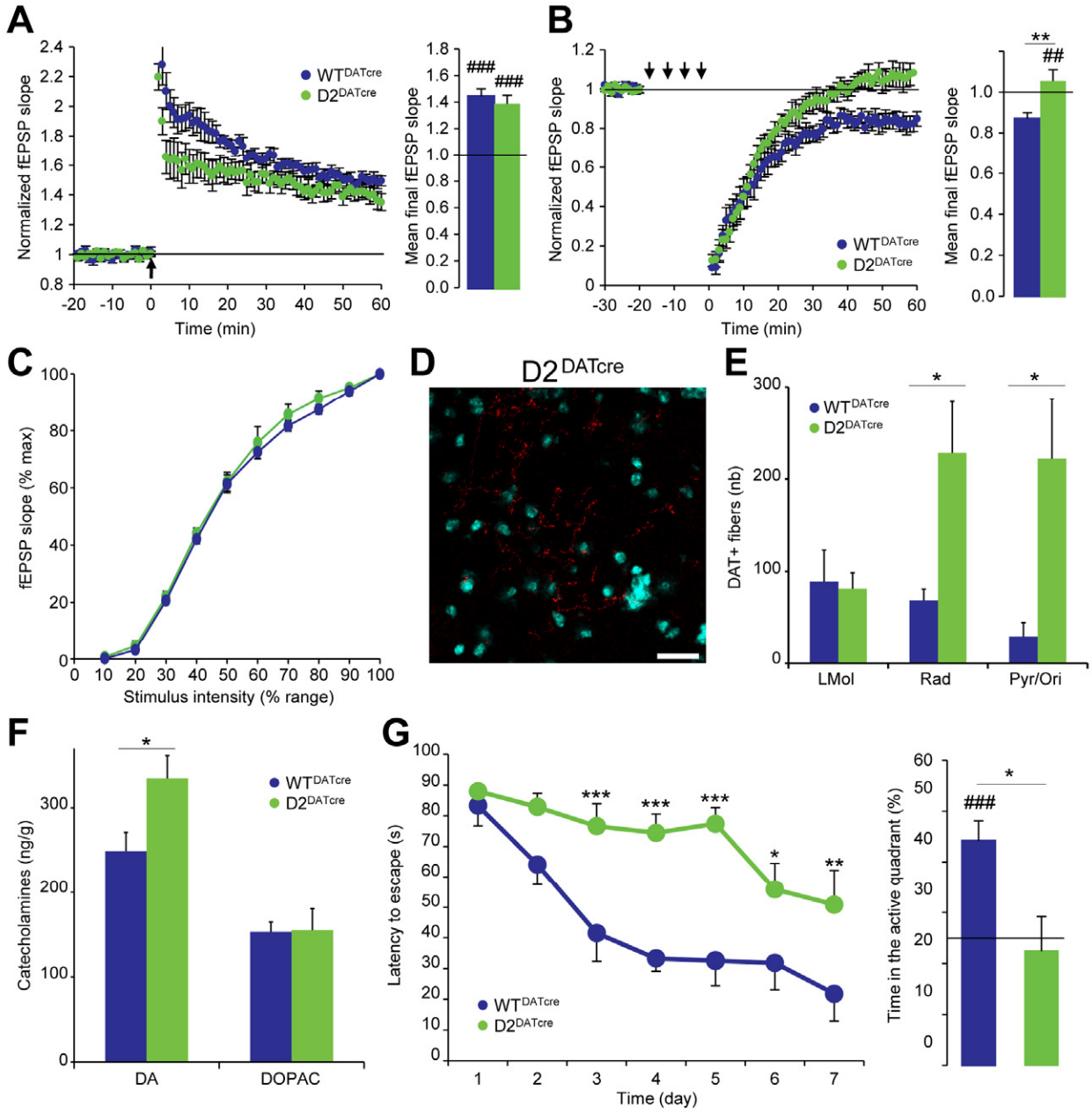
A
Normalized fEPSP slope
WT DATcre
D2 DATcre
Time (min)
Mean final fEPSP slope
###
###
B
Normalized fEPSP slope
WT DATcre
D2 DATcre
Time (min)
Mean final fEPSP slope
**
##
C
fEPSP slope (% max)
Stimulus intensity (% range)
D
D2 DATcre
E
DAT+ fibers (nb)
WT DATcre
D2 DATcre
*
*
LMol
Rad
Pyr/Ori
F
Catecholamines (ng/g)
WT DATcre
D2 DATcre
*
DA
DOPAC
G
Latency to escape (s)
WT DATcre
D2 DATcre
***
***
***
*
**
Time (day)
Time in the active quadrant (%)
*
###